INVESTIGAREA COMPORTĂRII LA TEMPERATURI RIDICATE ŞI A MECANISMULUI SINTERIZĂRII UNOR BETOANE BAZATE PE CENUŞĂ DE TERMOCENTRALĂ
INVESTIGATION OF HIGH TEMPERATURE BEHAVIOR AND SINTERING MECHANISM OF FLY ASH BASED CONCRETES

ANJA TERZIĆ [1]*, LJUBIŠA ANDRIĆ[2], MILAN PETROV[2], ZAGORKA RADOJEVIĆ[1], LJILJANA MILIČIĆ[1]
[1]*Institute for Material Testing, Vojvode Mišića Bl. 43, Belgrade, Serbia*
[2]*Institute for Technology of Nuclear and other Raw Mineral Materials, Franchet d'Esperey 86, Belgrade, Serbia*

Four types of refractory concretes were studied at various temperatures ranging from ambient to adopted maximal 1400°C. The concretes had same matrix composition: K concretes were based on corundum aggregate; B concretes were based on bauxite aggregate and chamotte filler; while K2 and B2 concretes had 30 % of fly ash replacement in bonding agent. Fly ash was mechanically activated by means of planetary ball mill. Samples were dried at 110°C during 24 hours to create standard specimens. Afterwards, the samples were preburned at 1100°C and subsequently subjected to compressive uniaxial creep test conducted at various temperatures (1200, 1300 and 1400°C). Thermal behavior was also investigated by dilatometry analysis starting from room temperature up to 1400°C. The evolution of the refractory concretes behavior from quasi-brittle to visco-plastic was investigated and correlated to their microstructure evolution induced by sintering process. The influence of the burning temperature and procedure duration on the concretes behavior is also discussed. Creep test and dilatometry analysis helped in defining of the sintering mechanism and its parameters, and additionally explained deformation nature of the refractory concretes.

Keywords: *sintering, thermal treatment, composites, thermal properties, environment*

1. Introduction

Fly ash as a by-product of the coal combustion process is used in a variety of engineering applications. The most common application of the fly ash is as replacement of portland cement in standard building concretes [1]. Despite the wide area of engineering branches where fly ash is applied as secondary raw material, the demands for new applications are being raised on daily basis. Today, worldwide annual production of coal fly ash is estimated at around 500 million tones [2]. As a result, huge amount of combusted waste in the form of fly ash, bottom ash and slag have been generated and, thus, the amount of coal fly ash has been increased throughout the world, while the disposal of this waste product has become a serious environmental problem [3, 4]. The new forms of utilization for this waste material have to be found. Since fly ash shows adequate behavior at elevated temperatures there is a possibility that it can be used as a component in refractory concretes [5, 6].

Refractory concretes are unshaped materials designed similar to standard building concretes. Refractory concretes are employed in construction of monolithic elements of metallurgical furnaces and in structures undergoing cyclic thermal loadings. For instance, refractory concretes are used as wearing or security lining in blast furnace, as the security lining in steel making ladle, and in electricity producing reactors [7]. A number of factors influence the deterioration of refractory concretes: oxidation due to high temperature and air interaction, erosion induced by movement of molten material, microstructure differential expansion, and thermo-mechanical stress induced by the thermal gradient [8]. The failure mechanism of refractory concrete is significantly more complex than that of building concrete. The sintering process is phenomenon which distinguishes difference between standard and refractory concrete. While mechanical characteristics such as compressive and tensile strength are most important for standard concretes [9], in the investigation of refractory concretes accent is on materials behavior during exposure to elevated temperature and on the type of sintering mechanism. In this work, behavior of the refractory concretes during exposure to elevated temperatures was investigated by two methods: creep resistance and dilatometry analysis.

Refractory concretes are composed of refractory cement, high temperature-resistant aggregates, and minimum water content. Some other constituents, such as for example silica fume, or fly ash can be included in certain amounts in order to improve the flow-ability or other chemical or physical properties [10]. There is a considerable amount of literature on the sintering of fly ash

* Autor corespondent/*Corresponding author*,
E-mail: anja.terzic@institutims.rs.

highlighting the positive influence of the thermal treatment on the mineralogical, chemical and physical properties and justifying the application of fly ash in refractory concrete [11-15]. In order to improve the characteristics of the fly ash as component in the design of refractory concretes mechanical activation procedure has been applied. The mechanical activation of solid substance is accomplished by fine and ultrafine activation of the material in the specially designed high-energy mills [16]. The activated state of the non-organic material occurs as a result of the increase of the specific surface, high concentration of dislocations, and an increase of the atomic defects number in the activated material [17]. Activation is a complex physical-chemical process which brings about the increase of potential energy, chemical activity and surface reactivity of the system [18, 19].

The present paper reports original data on the experimental characterization and investigation of high-temperature behavior and sintering process of four different types of refractory concretes designed with addition of fly ash.

2. Description of experimental methods

The investigation was conducted on four types of refractory concretes: B1, B2, K1 and K2. Concrete specimens contained different portions and types of refractory aggregates: B concretes were designed with bauxite aggregate (calcinated bauxite, Sharad Enterprises, India) and chamotte filler (Factory "Šamot", Serbia) and K concretes contained corundum aggregate (fused alumina, MOTIM Fused Cast Refractories Ltd., Hungary). High aluminate cement (Secar 70/71, Lafarge, France) was applied as refractory bonding agent in all concretes. Fly ash was added in the composition of B2 and K2 mixtures. Mixtures of investigated concretes are given in Table 1.

The fly ash used in the investigation is a by-product of the combustion of lignite coal and it originates from the filter system of coal-fired power plant ("Nikola Tesla-Tent A", Serbia). The fly ash was collected directly from the filter and transported to a special closed silo. Used fly ash belongs to F-class with average grain size varying from several μm up to 2 mm [5]. The fly ash was mechanically activated by means of a laboratory mechanical activator, before mixing with refractory cement, in order to reduce the particle size and improve over-all characteristics of the ash [20-22]. Planetary ball mill type Retsch-PM 100 was applied in this investigation. The Retsch-PM 100 uses charge of 2 kg of stainless steel balls sizing 12 mm for milling. Material to media ratio during milling was 1:35. The activation period was 15 min. Fly ash particles fraction content after activation was analyzed by cyclo-sizer diffraction particle size analysis (Cyclo-sizer - Warman International LTD, Australia).

Theoretical principle of operation of conventional mechanical activator is as follows: activator operates at a constant speed due to the centrifugal force; processed material is being lifted and pushed towards the mill walls and from this position material falls at a parabolic path, becoming activated due to collisions with grinding bodies and other particles [23, 24]. In order to explain the activation procedure the number of activation cycles can be replaced with activation time (t). The mill rotates (g) revolutions per minute and the number of revolutions cycles of grinding balls is approximately equal to ($2g \cdot t$) [24]. At a constant operating speed the following equation is obtained:

$$R_t = R_0 \cdot k_0^{2gt} = R_0 \cdot k_0^{'t} \qquad (1)$$

Where: R_t is coarse particles content after time t, %; R_0 is coarse particles content at activation beginning t_0, %; k_0' is relative activation rate; g is gravity constant; t is activation time, h.

The number of cycles is replaced with

Table 1

Mix-design of the investigated refractory concretes.

	B1	B2	K1	K2
Fly ash	-	9 %	-	9 %
High aluminate cement	30 %	21%	30 %	21%
Corundum aggregate 3-5 mm 2-3 mm 1-2 mm 0.5-1mm 0-0.5 mm	-	-	(Σ 70%) 30 % 20 % 30 % 10 % 10 %	(Σ 70%) 30 % 20 % 30 % 10 % 10 %
Bauxite aggregate 4-6 mm 1-4 mm 0-1 mm Chamotte aggregate 23-33 μm	(Σ 70%) 10 % 50 % 30 % 10%	(Σ 70%) 10 % 50 % 30 % 10%	-	-
Water / (Cement + FA)	0.60	0.61	0.55	0.56

activation time since the duration of one cycle is only a small fraction of total activation time:

$$R_t = R_0 \cdot e^{-kt} \quad (2)$$

The capacity of the mill (Eq. 3) and consumed specific energy (Eq. 4) depend on the amount of processed material and activation period (*t*) [24]:

$$Q = \frac{G}{t} \quad (3)$$

Where: *Q* is capacity of activator, kg/h; and *G* is the amount of processed material, kg.

$$E = N \cdot t \quad (4)$$

Where: *E* is energy consumed during activation, kWh; and *N* is the power of the activator engine, kW.

Theoretical principle of planetary ball mill operation is based on principle of conventional mill, however planetary ball mill capacity is limited by gravity constant and the relation between acceleration (*a*) and gravitational acceleration (*g*), i.e. *a/g* corresponds to the Fraude number (F_r). The Fraude number is directly proportional with mill diameter (R_M) and circumferential velocity (ω_M), and inversely proportional with the gravity acceleration (*g*) [24]:

$$F_{r_M} = \frac{R_M \cdot \omega_M^2}{g} \quad (5)$$

Intensity of mechanical activation of particles directly depends on ball diameter (*d*), ball density (ρ), number and frequency of contacts between balls (f_n) and mechanical activation time (t).

$$\frac{t_M}{t_P} = \left(\frac{f_{n_P}}{f_{n_M}}\right) \cdot \left(\frac{d_M}{d_P}\right) \text{ and}$$

$$\frac{t_M}{t_P} = m^2 \sqrt{\frac{\rho_M}{\rho_P}} \quad (6)$$

Where: f_{np} and f_{nM} are number and frequency of ball contacts in activator; d_M and d_p are ball diameters, m; ρ_M and ρ_p are ball densities, kg/m^2; t_M and t_p are activation times, h; and *m* is proportionality factor.

Creep is plastic deformation of material which is time dependent at constant temperature and constant load. The rate of deformation is a function of material properties, exposure time, exposure temperature and applied structural load. General creep equation can be described as [25-27]:

$$\varepsilon_s = \frac{C \cdot \sigma^m}{d^c} \cdot \exp\left(-\frac{E_a}{kT}\right) \quad (7)$$

Where: ε_s ($d\varepsilon/dt$) is the rate of creep process; *C* is a constant dependent on the material and the creep mechanism; *m* and *c* are exponents dependent on the creep mechanism; E_a is the activation energy of the creep mechanism, KJ; σ is the applied stress, KN; *d* is the grain size of the material, mm; *k* is Boltzmann's constant, m^2 kg s^{-2} K^{-1}; and *T* is the temperature, K.

At high stresses the creep is controlled by the movement of dislocations. When a self diffusion occurs in a material, creep becomes dependent on the applied stress (*m* = 4 - 6) and independent on the grain size (*c* = 0) [28]. The diffusion coefficient is defined as [29, 30]:

$$K_d = K_0 \cdot \exp\left(-\frac{\Delta E_a}{RT}\right) \quad (8)$$

Where: K_d is the diffusion coefficient; K_0 is the maximum diffusion coefficient (at infinite temperature); E_a is activation energy of the creep process; and *R* is universal gas constant.

Equations (7) and (8) can be combined into equation - power law creep [25]:

$$\varepsilon_s = A_0 \cdot \sigma^n \cdot \exp\left(-\frac{\Delta E_a}{RT}\right) \quad (9)$$

Where: A_0 and *n* are constants; and ε_s is rate of creep process.

Pines' equation of sintering (can be applied for quantitative data processing for isothermal sintering process during secondary creep state [25]:

$$\frac{\Delta l}{l_0} = k \cdot t^n \quad (10)$$

Activation energy of the sintering process can be calculated using the following equation:

$$E_a = \frac{R \cdot T_1 \cdot T_2}{(T_1 - T_2)} \cdot \ln\left(\frac{v_{s1}}{v_{s2}}\right) \quad (11)$$

Where: *v* is the rate of sintering process (Δl is shrinkage of a sample; Δt is duration of shrinkage process) at temperatures T_1 and T_2.

For calculation of activation energy of the sintering process, an equation derived from Frenkel's model of sintering can be used [25]:

$$\frac{\Delta l}{l_0} = k \cdot T^2 \cdot \exp\left(-\frac{E}{R \cdot T}\right) \quad (12)$$

Creep testing was conducted on 50 x 50 mm cylindrically shaped samples [31]. Each sample had a 5 mm wide hole drilled in its center. The samples were preburned at 1100ºC. Compressive creep apparatus (Netzsch, Germany) was used in the creep investigation. Samples were heat-treated at a constant rate of 5°C/min from room temperature up to testing temperature. During investigation samples were putted under constant compressive load (0.2 MPa). Testing was performed at 1200, 1300 and 1400ºC with 30

hours delay at each temperature. During this period secondary state creep was reached. Dilatometry analysis was conducted on a Baehr GmbH DIL 802 s apparatus up to 1400°C with heating rate of 10 °/min. All analyses were recorded at a cooling rate of 10 °/min.

3. Results, interpretation and discussion

Table 2 and Figure 1 show results obtained after mechanical activation of fly ash, in the planetary ball mill.

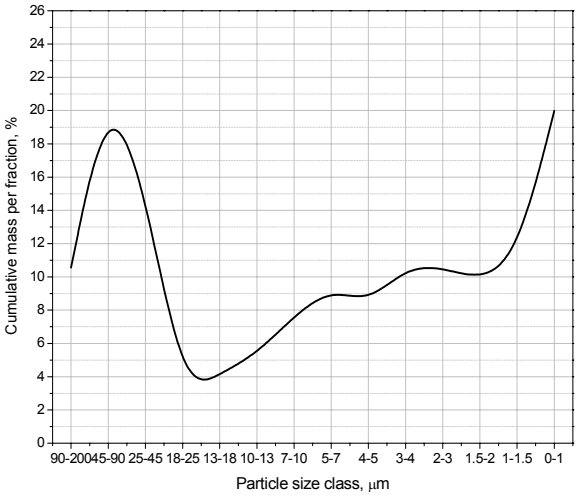

Fig. 1 - Diagram of the granulometric composition of the activated ash.

The main grain size composition parameters are: d_{50} - mean particle diameter; d_{95} - sieve opening through which passes 95 % of the activated product; n - direction coefficient; and S - specific surface area. Cumulative characteristics of the size of activated material can be described by functional dependency between the mean diameter, cumulative oversize - R, and undersize - D. This dependence is usually described by the Rosin-Rammler equation [24, 32]:

$$R = 100e^{-\left(\frac{d}{d_{50}}\right)^n} \quad (13)$$

Where: *R* is cumulative oversize; %; e is basis of natural logarithm (e= 2,718); *d* is sieve opening; mm; d_{50} is mean grain diameter; mm.

By performing a double logarithm of Eq. (13), a new equation in the coordinate system (log (*d*); log(log(100/*R*))) is obtained which represents a straight line equation with the direction coefficient- *n* [24]:

$$n = \frac{\log\log\frac{100}{R_1} - \log\log\frac{100}{R_2}}{\log d_1 - \log d_2} \quad (14)$$

Parameter d_{95} can be calculated using the Eq. (13), i.e by multiplying it with natural logarithm:

$$d_{95} = e^{\left(\frac{n\ln d_{50} + \ln\ln 100 - \ln\ln R}{n}\right)} \quad (15)$$

Specific surface area can be calculated as:

$$S_t = \frac{6.39}{\rho \cdot d'} e^{\frac{1.795}{n^2}} \quad (16)$$

Where: *S* is theoretical specific surface area; m^2/kg; d_{50} and *n* are Rosin-Rammler equation parameters; e is basis of natural logarithm (e =2.718); and ρ is density; kg/m^3

Parameters of fly ash activation obtained with from Eq. (13)-(16) are given in Table 3.

The refractory concrete specimens (B1, B2, K1 and K2) were prepared according to the mixture design presented in Table 1 and following the standard methods for sample shaping and curing [33]. Analysis of chemical constituents existing in concrete samples was performed by means of X-ray fluorescence (XRF) technique - XRF spectrophotometer ED 2000 – Oxford [34]. The results of the chemical analysis are given in Table 4.

Values of investigated physical, mechanical and thermal properties of refractory concretes, according to [35-40], are given in Table 5.

Table 2

The grain size composition of the fly ash after mechanical activation

Size class, μm	M, %	Oversize – R, %	Undersize –D,%
18-25	1.85	1.85	100.00
13-18	3.19	5.04	98.15
10-13	5.78	10.82	94.96
7-10	6.59	17.41	89.18
5-7	10.99	28.40	82.59
4-5	11.34	39.74	71.60
3-4	7.46	47.20	60.26
2-3	9.05	56.25	52.80
1.5-2	11.11	67.36	43.75
1-1.5	6.53	73.89	32.64
0-1	26.11	100.00	26.11
Total	100.00		

Table 3

Parameters of fly ash mechano-activation

Fly ash sample	Duration of mechano activation, min	Mean grain diameter d_{50}, μm	d_{95}, μm	Specific surface S, m^2/g	Specific energy consumption, W_m, kWh/kg	Agglomeration tendency
Initial sample	-	82.66	334.33	0.67	-	-
Activated sample	15	5.00	17.00	3.44	0.95	low

Table 4

Chemical composition of the refractory concrete samples

Oxides, wt.%	B1	B2	K1	K2
Al_2O_3	61.72	60.53	94.02	90.62
SiO_2	20.97	20.07	0.08	0.09
CaO	8.96	9.26	5.25	6.91
MgO	0.55	0.75	0.05	1.03
Fe_2O_3	1.92	2.57	0.09	0.1
Na_2O	0.06	0.07	0.34	1.0
K_2O	0.98	1.56	-	-
TiO_2	2.64	2.93	0.02	0.03
LoI	2.11	2.62	0.15	0.22

Table 5

Physical, mechanical and thermal properties of refractory concretes

Property of the material:	B1	B2	K1	K2
Bulk density at 20/1400°C, kg/m^3 [35]	2460/2050	2490/2060	2830/2440	2900/2450
Apparent porosity at 20/1400°C, % [36]	10.3/28.9	9.8/27.8	10.1/28.5	9.6/27.2
Refractoriness [37]	20SK /1450°C	20SK/1450°C	34SK/1755°C	34SK/1755°C
Refractoriness under load of 0.2 MPa, Ta/Te, ºC [38]	1300/1570	1300/1570	1450/1600	1450/1600
Compressive strength at 20/1400°C , MPa [39]	45.0/20.1	48.3/21.4	59.2/25.3	61.6/27.5
Flexural strength at 20/1400°C , MPa [40]	15.6/6.1	15.9/6.5	17.8/8.5	19.0/9.0

The initial refractory concrete samples (at 20°C) and samples after burning at 1400°C were examined by means of optical microscope JENAPOL (Carl Zeiss, Jena, Germany) equipped with a system for microphotography (Micro-photo System STUDIO PCTV; Pinnacle Systems, Mountain View, CA), (Figures 2-9).

Investigated refractory concretes have heterogeneous microstructure: aggregate particles are surrounded by fine cement matrix. In the microphotograph recordings of B2 and K2 concretes, in whose mixture fly ash was included, it can be noticed that empty vacancies were filled out by small micronized ash particles. Pores of various sizes are present in all samples. Higher porosity is noticed in B samples than in K samples. Towards higher temperature, certain structural changes are taking place: formation of liquid phase and emersion of initially formed mullite crystals. The microstructure of samples after burning at 1400ºC is different than the microstructure of initial samples: it is more compact and the pores are smaller as the consequence of sintering process.

Creep curves, obtained for investigated refractory concretes B1, B2, K1 and K2, following the described standard procedure [31] are given in Figures 10 and 11.

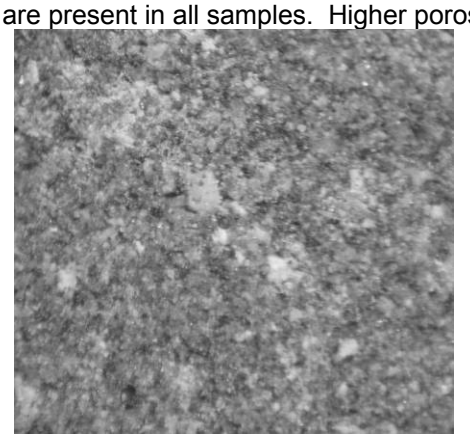

Fig. 2- Concrete sample B1 recorded at 20°C.

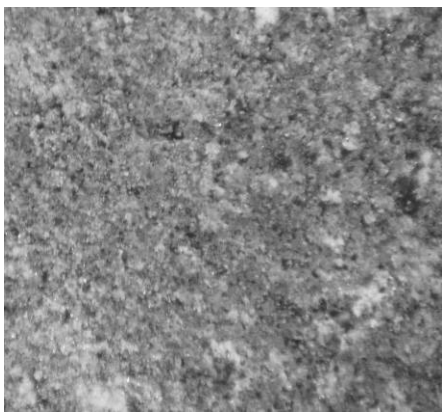

Fig. 3 - Concrete sample B2 recorded at 20°C.

Fig. 4 - Concrete sample B1 recorded at 1400°C.

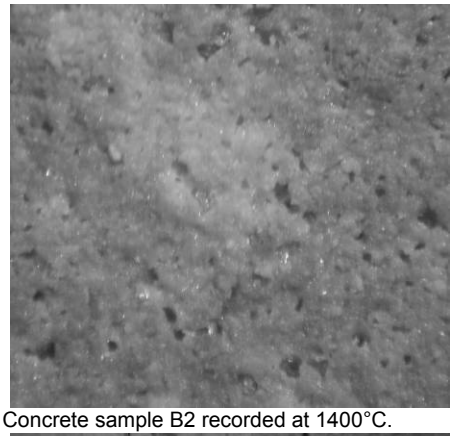

Fig. 5 - Concrete sample B2 recorded at 1400°C.

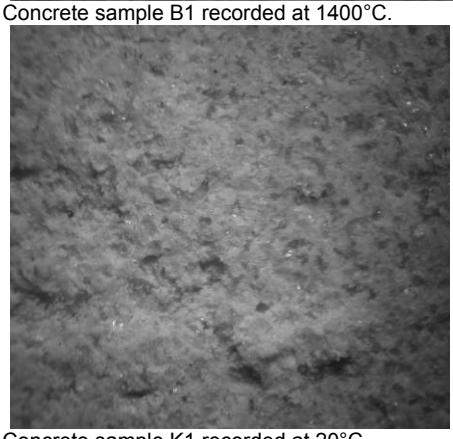

Fig. 6 - Concrete sample K1 recorded at 20°C.

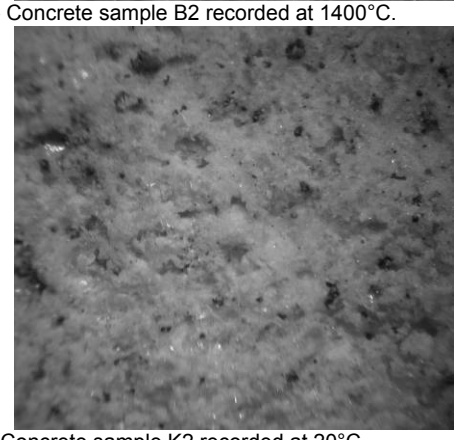

Fig. 7- Concrete sample K2 recorded at 20°C.

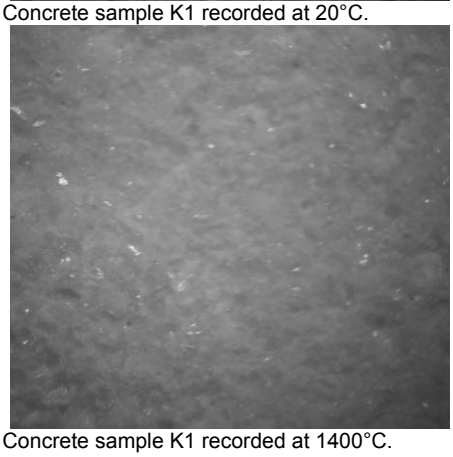

Fig. 8 - Concrete sample K1 recorded at 1400°C.

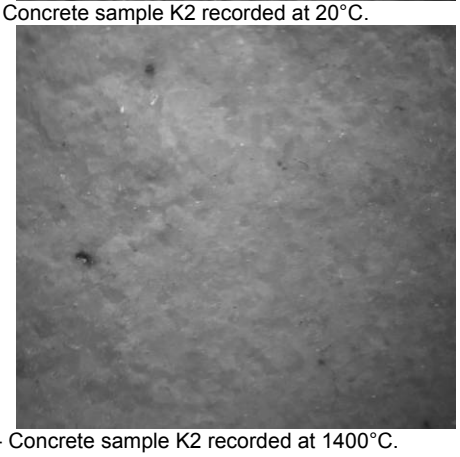

Fig. 9 - Concrete sample K2 recorded at 1400°C.

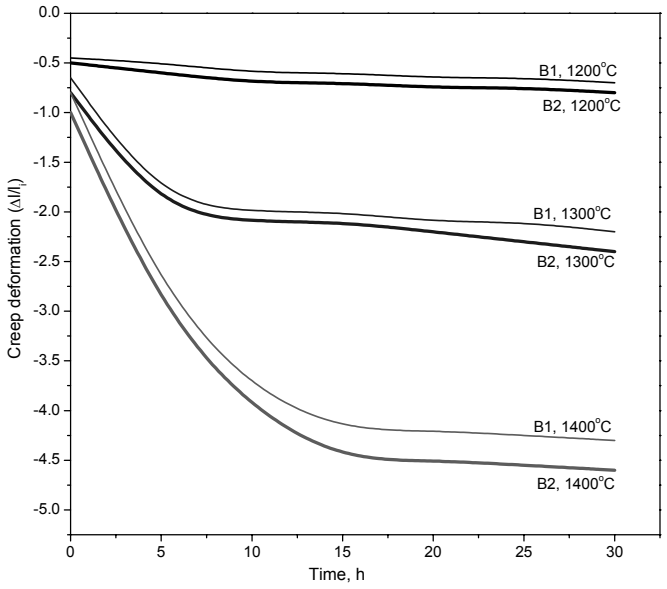

Fig. 10 - Creep curves for B1 and B2 refractory concretes.

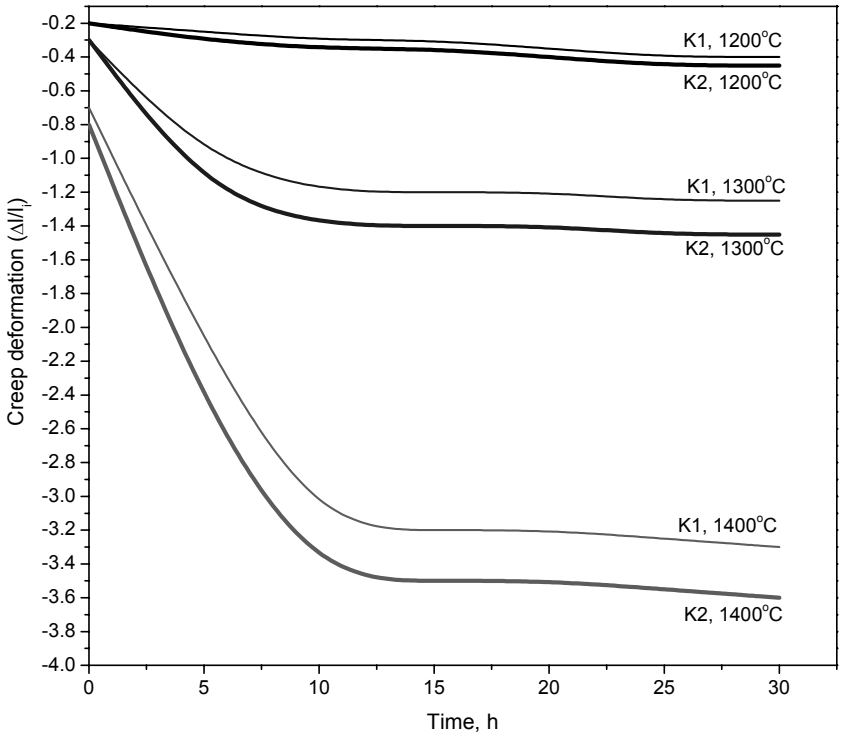

Fig. 11 - Creep curves for K1 and K2 refractory concretes.

The deformation is time dependent, in conditions of the constant applied load (0.2 MPa) and temperatures. Diagrams show deformation recorded above 1200°C, because deformations which were present at temperatures below 1200°C are irrelevant for sintering mechanism quantification. Investigation was conducted at three temperatures: 1200, 1300 and 1400°C with time delay of 30 hours at each temperature. Deformation l_0 which is a consequence of shrinkage occurred during heating from room temperature up to 1200°C is present at the beginning of the investigation (0 hours). Since the change in characteristic deformation (height of sample - l_i) is recorded value, the creep deformation is calculated as relative change of measured dimensions $\Delta l/l_i$

Sintering process was investigated during secondary stage of creep when creep deformation is minimal and time independent. Namely, that state relates to isothermal sintering under compressive load, therefore sintering equations can be applied on results obtained during creep investigation.

It can be noticed that maximal deformation occurs at the highest temperature of investigation - temperature 1400ºC for all four concrete types. Deformations are 4.5; 4.4; 3.6; and 3.3 % for concretes B1, B2, K1 and K2, respectively. The creep deformation increases with the temperature of treatment investigation for each investigated concrete type. The shape of creep curves is similar at all three considered applied temperatures. Primary creep state lasts for approximately 5 hours for all concrete types. Afterwards, primary creep is exceeding towards secondary state of creep. Transition of primary into secondary creep is not clearly noticeable at 1200ºC. However, this transition becomes distinctly visible for 1300 and 1400ºC, and it occurs at approximately 15 hours. The onset of tertiary state was not detected during 30 hours of investigation.

It is assumed that refractory concretes show visco-plastic behavior, therefore the fine matrix, which is situated in inter-aggregate space within concrete, is changing with increasing temperature and above 1200ºC it proceeds into liquid phase. Thus, deformation which occurs at temperatures above 1200ºC can be approximated by means of visco-plastic model. At high temperatures (1400ºC and above) secondary mullite crystallizes from liquid phase. Newly formed mullite gives more resistance to deformation at high temperatures by structurally reinforcing of the material. Fly ash additionally contributed to the formation of mullite at high temperatures, making final deformations of B2 and K2 samples smaller than deformations of K1 and B1 [5]. By observing the creep diagrams two rules can be established: (1) deformation is smaller in case of corundum based concretes; and (2) deformation is smaller in case of concretes with addition of activated fly ash. First rule can be explained by high refractoriness and hardness of corundum aggregate, and second by better packing of concrete microstructure provided helped by activated ash [6].

In Table 6, absolute values of total relative

Table 6

Isothermal sintering deformation of refractory concretes measured by creep test

	Deformation $\Delta\varepsilon = \frac{\Delta l}{l_{30}} - \frac{\Delta l}{l_5}$		
	at 1200ºC	at 1300ºC	at 1400ºC
B1	0.2	0.4	1.5
B2	0.2	0.3	1.6
K1	0.15	0.25	1.1
K2	0.15	0.25	1.2

Table 7

Isothermal sintering parameters obtained from creep investigation

T, ºC	n	$v \cdot 10^{-3}$, mm/min	Mechanism of sintering	Ea, kJ/mol
B1				
1200	0.35	0.13	diffusion along the grain boundary	
1300	0.69	0.27	plastic-viscous flow	$Ea_{1200\text{-}1300}$ =263.5
1400	0.62	1.00	plastic-viscous flow	$Ea_{1300\text{-}1400}$ =167.1
B2				
1200	0.30	0.13	diffusion along the grain boundary	
1300	0.71	0.20	plastic-viscous flow	$Ea_{1200\text{-}1300}$ =247.2
1400	0.60	1.10	plastic-viscous flow	$Ea_{1300\text{-}1400}$ =128.3
K1				
1200	0.60	0.10	diffusion along the grain boundary	
1300	0.69	0.17	plastic-viscous flow	$Ea_{1200\text{-}1300}$ =363.0
1400	0.62	0.73	plastic-viscous flow	$Ea_{1300\text{-}1400}$ =150.1
K2				
1200	0.58	0.10	diffusion along the grain boundary	
1300	0.68	0.17	plastic-viscous flow	$Ea_{1200\text{-}1300}$ =363.0
1400	0.60	0.80	plastic-viscous flow	$Ea_{1300\text{-}1400}$ =141.3

dimensional change of concrete samples are given for each temperature - 1200, 1300 and 1400ºC.

Sintering process and its parameters during secondary state of creep were investigated using the results of dimensional changes of four different types of refractory concretes (B1, B2, K1 and K2) obtained during creep test (Figs. 10 and 11 and Tab. 6.). Using equations (15), (16) and (18) the approximate coefficient of reaction mechanism (*n*), rate of sintering (*v*), and activation energy (*E*a) have been calculated. Table 7 shows the quantitative values (*n*, *v, E*a, and qualitative parameter (mechanism) of the sintering process investigated at temperatures of 1200, 1300 and 1400 ºC.

The most dominant sintering mechanism is plastic-viscous flow as it was previously concluded. Diffusion along the grain boundary, as sintering mechanism, appears at the lowest temperature of the investigation (1200ºC). Addition of activated fly ash increased the rate of sintering.

The diagrams of non-isothermal sintering recorded by dilatometer are given in Figures 12-15. Shorter duration of shrinkage interval for samples B2 and K2 points out to the faster sintering process, as it was previously assumed.

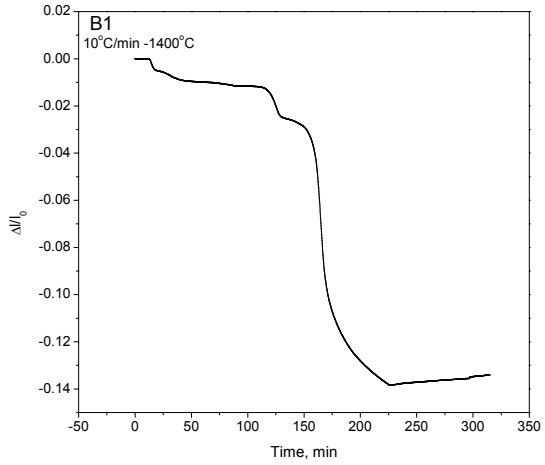

Fig. 12 - Dilatometry curve for B1 concrete.

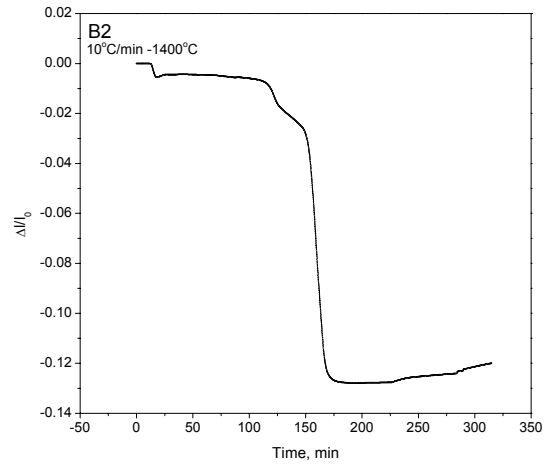

Fig. 13 - Dilatometry curve for B2 concrete.

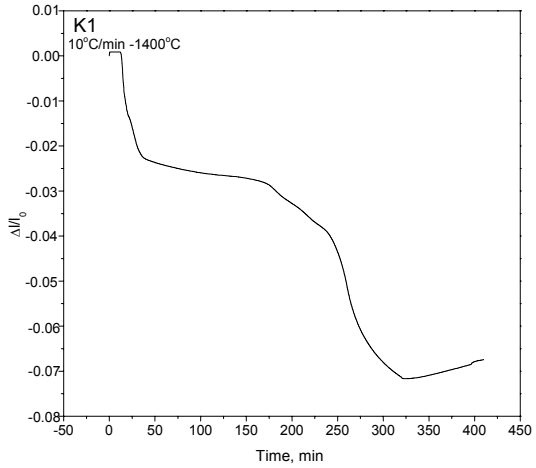

Fig. 14 - Dilatometry curve for K1 concrete.

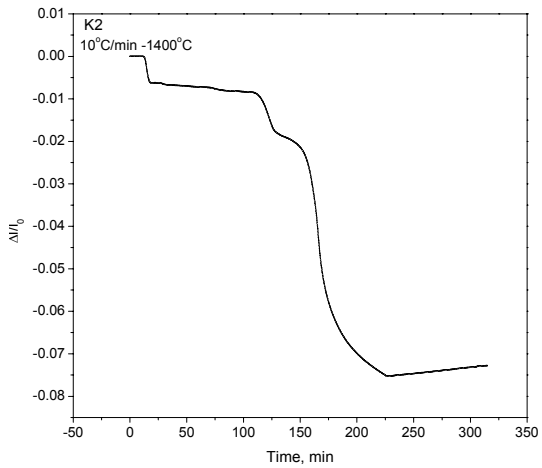

Fig. 15- Dilatometry curve for K2 concrete.

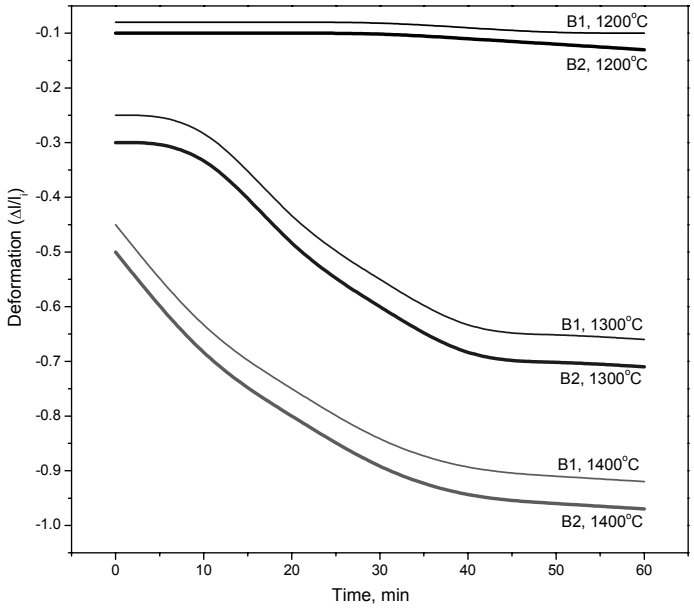

Fig. 16 - Isothermal dilatometry curves for B1 and B2 concretes.

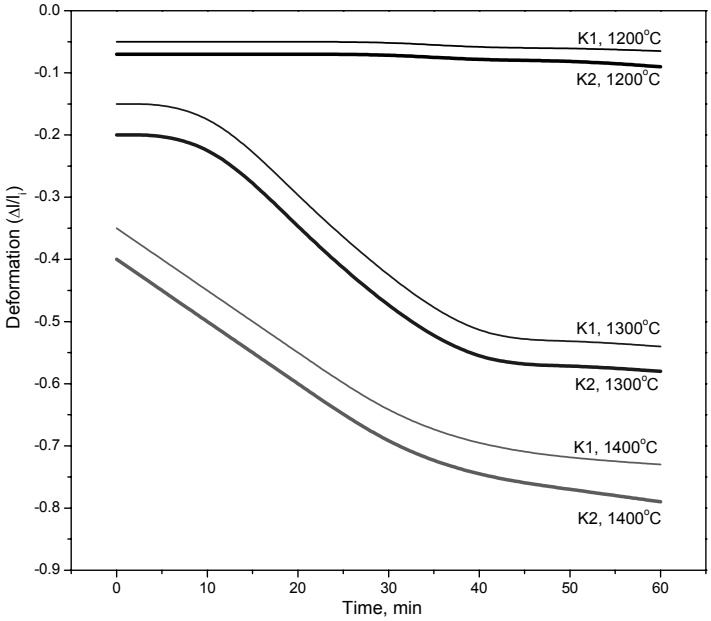

Fig. 17 - Isothermal dilatometry curves for K1 and K2 concretes.

Dilatometry analysis was also conducted in condition of isothermal sintering at three temperatures - 1200, 1300 and 1400°C with isothermal delay of 60 minutes at each temperature. The diagrams are given in Figures 16 and 17.

As in the creep investigation, curves obtained from dilatometry analyses pointed out that registered deformations are smaller in case of corundum based concretes than in bauxite concretes. Also, deformation is smaller in case of concretes with addition of activated fly ash.

Absolute values of total relative dimensional changes of concrete samples are calculated for each temperature of investigation - 1200, 1300 and 1400 ºC (Table 8).

Using equations (15), (16) and (18), approximate coefficient of reaction mechanism, rate of sintering and activation energy were calculated, as in the case of creep testing. Table 9 shows quantitative and qualitative parameters of isothermal sintering investigated by dilatometry analysis at temperatures 1200, 1300 and 1400ºC.

Obtained values for the coefficient *n* point out that predominant mechanism of the sintering is plastic-viscous flow. At lowest temperature of investigation (1200°C), diffusion along the grain boundary as sintering mechanism is recorded, as in the case of creep investigation. Dilatometry analysis also proved that addition of activated fly ash increased the rate of sintering, i.e. sample K2 and B2 had higher values of sintering rate than K1 and B1. Values *n*, *v* and *E*a differ from adequate values obtained during creep investigation because testing conditions also varies. These differences are normal. However, results of both dilatometry and creep investigation agreed concerning sintering mechanism and highlighted the viscous behavior of refractory concretes at high temperatures.

4. Conclusions

Corundum and bauxite based refractory concretes, with and without addition of activated fly ash, have been studied by uniaxial compression creep test and dilatometry, from room temperature up to 1400°C. The material behavior as well as the influence of the activated fly ash and firing conditions has been analyzed. Over-all behavior of investigated concretes approved their high-temperature application, and that the addition of mechanically activated fly ash highlighted the possibility of obtaining new refractory concretes with advanced characteristics. The major results are summarized below.

Table 8

Isothermal sintering deformation of refractory concretes measured by dilatometry

	Deformation $\Delta\varepsilon = \frac{\Delta l}{l_{30}} - \frac{\Delta l}{l_5}$		
	at 1200ºC	at 1300ºC	at 1400ºC
B1	0.03	0.41	0.27
B2	0.02	0.41	0.28
K1	0.02	0.38	0.29
K2	0.015	0.39	0.30

Table 9

Isothermal sintering parameters obtained by dilatometry investigation

T, ºC	n	$v \cdot 10^{-3}$, mm/min	Mechanism of sintering	Ea, KJ/mol
B1				
1200	0.40	0.6	diffusion along the grain boundary	
1300	0.66	2.2	plastic-viscous flow	$Ea_{1200\text{-}1300}$ =339.1
1400	0.60	7.4	plastic-viscous flow	$Ea_{1300\text{-}1400}$ =240.1
B2				
1200	0.39	0.4	diffusion along the grain boundary	
1300	0.87	2.2	plastic-viscous flow	$Ea_{1200\text{-}1300}$ =317.2
1400	0.60	7.6	plastic-viscous flow	$Ea_{1300\text{-}1400}$ =228.0
K1				
1200	0.67	0.4	diffusion along the grain boundary	
1300	0.65	3.6	plastic-viscous flow	$Ea_{1200\text{-}1300}$ =393.0
1400	0.62	5.8	plastic-viscous flow	$Ea_{1300\text{-}1400}$ =200.5
K2				
1200	0.54	0.3	diffusion along the grain boundary	
1300	0.69	3.2	plastic-viscous flow	$Ea_{1200\text{-}1300}$ =372.0
1400	0.67	6.0	plastic-viscous flow	$Ea_{1300\text{-}1400}$ =192.3

Mechanical activation of the fly ash influenced its microstructural characteristics and the energy state. Additionally, activation induced the increase in reactivity of the fly ash as raw material and changes in its mineralogical composition followed by the deterioration of the crystallinity. The significant decrease of the particle size after the mechanical activation in planetary ball mill can be ascribed to the strain increase due to the friction forces as well as the compression and impact forces during the mechanical activation. The samples activated in the planetary mechanical activator showed no tendency to create the agglomerations. Mechanically activated ash was successfully applied in refractory concretes and the characteristics of the concretes were further investigated.

Investigation of isothermal sintering by means of creep test and dilatometry at three constant temperatures (1200, 1300 and 1400ºC) showed that corundum samples have smaller deformation at all applied temperatures than bauxite samples due to higher refractoriness and hardness of aggregate. Addition of the activated fly ash increased the rate of sintering in both concretes. Two sintering mechanisms were noticed during investigation by means of both methods: diffusion along the grain boundary at 1200ºC, and plastic-viscous flow at 1300 and 1400ºC. Thus, the concretes exhibit quasi-brittle behavior at room temperature, but with temperature increasing above 1200ºC and initiation of sintering process concretes start showing viscous behavior. Approximate values of activation energy for temperature intervals 1200-1300/1300-1400ºC are 263.5/167.1, 247.2/128/3, 263.0/150.1, 363.0/141.3 kJ/mol for B1, B2, K1 and K2 concretes, respectively. The results of creep test were adopted as more accurate.

The viscous behavior of investigated concretes can be correlated to micro structural and phase composition changes of the material. In particular, the presence of activated fly ash lowered the temperature at which the viscous phenomena are present and induced increasing of the sintering rate. By speeding up the sintering process and possibly decreasing the sintering temperature, a certain save in the thermal energy necessary for the refractory material production can be achieved Thus, it should be highlighted that addition of activated ash indirectly influences and benefits the production of refractory concrete by making the technology more economical and thermally sustainable.

Acknowledgements

This investigation was supported by Serbian Ministry of Education, Science and Technological Development and it was conducted under following projects: 172057, 45008 and 34006.

REFERENCES

1. R. Chancey, P.Stutzman, M. Juenger, and D. Fowler, Comprehensive phase characterization of crystalline and amorphous phases of a Class F fly ash, Cement and Concrete Research 2010, **40**,146.
2. I. Acar, and M.U. Atalay, Characterization of sintered class F fly ashes, Fuel 2013, **106,** 195.
3. M. Erol, S. Küçükbayrak, and A. Ersoy-Meriçboyu, Characterization of coal fly ash for possible utilization in glass production, Fuel 2007, **86**, 706.
4. I. Jovanović, S. Bugarinović, D. Urošević, L. Obradović, and S. Magdalinović, Characteristics of Portland cement containing fly ash treated by different physical methods, Romanian Journal of Materials 2013, **43**(3), 263.
5. A.Terzić, Lj.Pavlović, Z. Radojević, V.Pavlović, and V.Mitić, Novel Utilization of Fly Ash for High-temperature Mortars: Phase Composition, Microstructure and Performances Correlation, International Journal of Applied Ceramic Technology 2013, DOI:10.1111/ijac.12135.
6. A.Terzić, Lj.Pavlović, N.Obradović, V.Pavlović, J.Stojanović, Lj.Miličić, Z.Radojević, and M. Ristić, Synthesis and Sintering of High-temperature Composites Based on Mechanically Activated Fly Ash, Science of Sintering, 2012, **44** (2) 135.
7. E.Ouedraogo, M. Roosefid, N.Prompt, and C.Deteuf. Refractory concretes uniaxial compression behaviour under high temperature testing conditions, Journal of the European Ceramic Society, 2011, **31,** 2763.
8. F. Simonin, C. Olagnon, S. Maximilien, and G. Fantozzi, Roomtemperature quasibrittle behaviour of an aluminous refractory concrete after firing, Journal of the European Ceramic Society 2002, **22**, 165.
9. K. Janković, G. Ćirovic, D. Nikolić, and D. Bojović, Mechanical Properties of Ultra High Performance Self Compacting Concrete with Different Mineral Admixtures, Romanian Journal of Materials 2011, **41**(3), 211.
10. A. Tomba Martinez, A.Luz, M. Braulio, and V. Pandolfelli, Creep behavior modeling of silica fume containing Al_2O_3–MgO refractory castables, Ceramics International 2012, **38**(1), 327.
11. M. Erol, S. Kucukbayrak, A. Ersoy-Mericboyu, Characterization of sintered coal fly ashes, Fuel 2008, **87**, 133.
12. M. Erol, S. Kucukbayrak, A. Ersoy-Mericboyu, Comparison of the properties of glass, glass-ceramic and ceramic materials produced from coal fly ash, Journal of Hazardous Materials 2008, **153**, 418.
13. J. Biernacki, A. Vazrala, H. Leimer HW, Sintering of a class F fly ash, Fuel 2008, **87**, 782.
14. M. Ilic, C. Cheeseman, C. Sollars, J. Knight, Mineralogy and microstructure of sintered lignite coal fly ash, Fuel 2003, **82**, 331.
15. E. Furlani, S. Bruckner, D. Minichelli, and S. Mashio, Synthesis and characterization of ceramics from coal fly ash and incinerated paper mill sludge, Ceramic International 2008, **34**, 2137.
16. R.Kumar, S. Kumar, and S.P. Mehrotra, Towards sustainable solutions for fly ash through mechanical activation, Resources, Conservation and Recycling 2007, **52,** 157.
17. J. Temuujin, R.P.Williams, and A. van Riessen, Effect of mechanical activation of fly ash on the properties of geopolymer cured at ambient temperature, Journal of Materials Processing Technology 2009, **209**, 5276.
18. O. Senneca, P.Salatino, R. Chirone, and L. Cortese, R.Solimene, Mechanochemical activation of high-carbon fly ash for enhanced carbon reburning, Proceedings of the Combustion Institute 2011, **33**, 2743.
19. S. Kumar, and R. Kumar, Mechanical activation of fly ash: Effect on reaction, structure and properties of resulting geopolymer, Ceramics International 2011, **37**, 533.
20. T. Inoue, and K. Okaya, Grinding mechanism of centrifugal mills – a simulation study based on the discrete element method, International Journal of Mineral Processing 1996, **44-45,** 425.

21. A.S. Kheifets, and I.J. Lin, Energy transformations in a planetary grinding mill - Part 1. General treatment and model design, International Journal of Mineral Processing 1996, **47,** 1.
22. K. Shinohara, B. Golman, T. Uchiyama, and M. Otani, Fine-grinding characteristics of hard materials by attrition mill, Powder Technology 1999, **103,** 292.
23. Lj. Andric, Lj. Pavlovic, S. Milosevic, and M. Petrov, Theoretical Principles of Mechanochemical Activation During the Operation of High-Energy Mechanoactivators, Powder Metallurgy Science & Technology Briefs 2001, **3**(6), 11.
24. Lj. Andrić, Mica – preparation and application, Monograph, 2006 (in Serbian).
25. M. Ristić, Principles of material science, SANU, Beograd, 1992 (in Serbian).
26. L.A. Diaz, and R. Torrecillas, Hot-bending strength and creep behavior at 1000–1400 °C of high alumina refractory castables with spinel, periclase and dolomite additions, Journal of the European Ceramic Society 2009, **29**(1), 53.
27. A.Tomba Martinez, A. Luz, M. Braulio, and V.Pandolfelli, Creep behavior modeling of silica fume containing Al_2O_3–MgO refractory castables, Ceramics International 2012, **38**(1), 327.
28. R. Twiss, and M. Moores, Structural Geology, W.H. Freeman & co (6th ed.), 2000.
29. A. Terzić, and Lj. Pavlovic, Quantitative Fformulation of Mechanism of Sintering Process During Creep Deformation of Refractory Concrete, Science of Sintering 2009, **41**(1), 49.
30. A.Terzić, and Lj.Pavlović, Correlation among sintering process, porosity, and creep deformation of refractory concrete, Journal of Materials Science 2009, **44**(11), 2844.
31. xxx, Serbian Standard: SRPS EN 993-9:2009 - Methods of testing dense shaped refractory products - Part 9: Determination of creep in compression.
32. Lj. Andrić, A.Terzić, Z.Aćimović-Pavlović, Lj. Pavlović, and M. Petrov, Comparative Analysis of Process Parameters of Talc Mechanical Activation in Centrifugal and Attrition Mill, Physicochemical Problems of Mineral Processing 2013, **50** (2), 433. http://dx.doi.org/10.5277/ppmp140202
33. xxx, Serbian Standard: SRPS EN 1402-5:2009 - Unshaped refractory products - Part 5: Preparation and treatment of test pieces.
34. xxx, Serbian Standard: SRPS EN ISO 12677:2012 - Chemical analysis of refractory products by X-ray fluorescence (XRF).
35. xxx, Serbian Standard: SRPS EN 993-2:2009 - Methods of test for dense shaped refractory products - Part 2 : Determination of true density
36. xxx, Serbian Standard: SRPS EN 993-1:2009 - Methods of test for dense shaped refractory products - Part 1: Determination of bulk density, apparent porosity and true porosity
37. xxx, Serbian Standard: SRPS B.D8.301:1974 - Refractories - Determination of pyrometric cone equivalent (refractoriness)
38. xxx, Serbian Standard: SRPS EN ISO 1893:2010 - Refractory products - Determination of refractoriness under load - Differential method with rising temperature
39. xxx, Serbian Standard: SRPS EN 993-5:2009 - Methods of test for dense shaped refractory products - Part 5: Determination of cold crushing strength
40. xxx, Serbian Standard: SRPS EN 993-6:2009 - Methods of test for dense shaped refractory products - Part 6: Determination of modulus of rupture at ambient temperature

****

MANIFESTĂRI ŞTIINȚIFICE / SCIENTIFIC EVENTS

ICCMATS 2014 International Conference on Construction Materials and Structures - From 24 November 2014 to 26 November 2014 , Johannesburg, South Africa

Theme:

The ICCMATS 2014 conference is organized by the University of Johannesburg (UJ) and Harbin Institute of Technology (HIT), China. The conference is the first of its kind on the African continent.

The conference aims at providing a platform for articulation of knowledge frontiers, developments and advancements in the domain of construction materials, structures and allied disciplines. Materials are the bridge between an engineering design to functional performance of a structure and eventually its service life or durability. Materials underlie the capabilities of any design and indeed define its limitations too. In this event, engineers, scientists, researchers, academicians, practitioners and professionals from materials, structures, mining, construction, transportation, and related fields come together for three days of engagement in cross-cutting presentations, discussions, and social capital.

The topics are herein outlined but other relevant titles will be considered. Papers may be based on experimental work, research and development, practice or industry application, case studies, innovations or other relevant work related to:

Cement, Concrete, Bitumen, Masonry, Steel, Timber, Special Building Materials, Polymers

Contact: http://www.iccmats-wits.co.za/

****